A Wearable Flexible Hybrid Electronics ECG Monitor

Mark Poliks, James Turner, Kanad Ghose, Zhanpeng Jin, Mohit Garg, Qiong Gui
Small-Scale Systems Integration & Packaging Center
Binghamton University, Binghamton, NY USA
mpoliks@binghamton.edu

Ana Arias & Yasser Kahn
Department of Electrical Engineering
University of California, Berkeley, Berkeley, CA USA
acarias@eecs.berkeley.edu

Mark Schadt & Frank Egitto
Research & Development
i3 Electronics, Inc., Endicott, NY USA
mark.schadt@i3electronics.com

Abstract—Flexible hybrid electronics (FHE) integrate both traditional printed circuits, solder assembled standard and thinned silicon chips along with printable electronic materials and sensors. The combination results in high performance from thin, light weight, flexible devices that potentially could be manufactured at low cost. In this paper, flexible hybrid electronics technology is being used to develop a wearable ECG and skin temperature monitor. All components and materials were commercially available, and all fabrication processes were executed in manufacturing environments. The monitor is composed of a flexible polyimide substrate with printed ECG electrodes, a printed thermistor, and connecting traces printed on one surface, and the electronic components mounted on other. Both sides have copper metal circuits connected by copper plated through hole vias (THV). ECG signals are amplified, preconditioned and wirelessly transmitted via Bluetooth to a nearby handheld mobile phone or computer. The wearable monitor is 2x2 inches in size and has been demonstrated to produce high fidelity ECG signals at the host from both certified archived human ECG signals and ECG signals from human volunteers. The monitor reproduced the archived signals at the host from which a set of clinical parameters were calculated that closely matched those of the archived signals. Manufacturing challenges and device reliability will be discussed. Current work includes building upon this platform and integration of other monitoring and sensor devices included those that monitor for biomarkers in sweat. This work was sponsored by the NanoBio Manufacturing Consortium administered by the Flextech Alliance and funded by the US Air Force Research Laboratory.

Keywords - BioCompatible and Medical Packaging, BioSensor Packaging, Flexible Substrates & Interconnection Solutions, Wearable and Medical Electronics, Interconnects for BioMedical, Novel Assembly Technologies.

I. INTRODUCTION

Flexible hybrid electronics (FHE) is exploiting the growing demand for wearable electronics of all sorts. This trend is especially strong with respect to health and fitness monitoring, detection and diagnosis of specific medical conditions, and fatigue and alertness assessment. These devices are, of course, leveraging the technological advances in wireless communications and the rapidly growing capabilities to utilize silicon based electronics attached to mechanically flexible and in some cases conformal substrates. FHE integrates solder attached silicon electronics along with printable materials and sensors onto flexible substrates [1,2].

ECG electrodes can be of various types. Conducting gel or wet electrodes that connect a metal electrode with the skin via an ionic gel are highly developed and are the standard of current medical methods. Dry electrodes are being developed that place a conducting solid or foam directly on the skin, or impale the skin with microneedles [3, 4]. Insulating or capacitive coupled electrodes are also being developed that insulate the electrode and the skin with a high dielectric material [5, 6]. While the dry and insulating electrodes have advantages, their use is not yet standardized in part due to motion artifacts and increased noise levels [7]. Thus, we chose to initially use gel electrodes to make direct comparisons between our results and those of certified archive ECG signals [8]. One of the major challenges is powering wearable sensors to allow long-term monitoring [1, 9].

The overarching goal of our project is to develop a "Band-Aid" like monitor for human biometric parameters, particularly cardiac function and assessment, and skin temperature. Ongoing work is developing specialized circuitry with the goal of improving capacitive coupled electrodes in part to insure that under no circumstances is more than 10 microamperes injected into the human body. Being a manufacturing project, all components must have stable certified supply lines. All human testing was done in

full compliance with our protocol approved by the Binghamton University's Internal Review Board. The objective of this work is to develop a wearable Biometric Human Performance Monitor (BHPM) for recording parameters such as electrocardiograms (ECGs) and skin temperature. The device is configured as a 2"x2" patch worn on the chest. We are reporting here the development of the ECG sensor portion of the device which is fabricated using flexible hybrid electronics (FHE). The device is based on a two sided Kapton substrate using ECG conducting gel electrodes printed with gold ink on the sensor side of the Kapton and with the electronic components attached to the other side. The components are attached using a low temperature soldering process. The two sides are connected by copper plated through hole vias (THVs). The ECG signals are conditioned by an analog chip with high gain, high and low band pass filtering, and a 60 Hz notch filter. The signals are digitized, processed, and wirelessly communicated to a host computer using a SoC. The device is intended to be single use and must be fabricated from commercially available components with well-established supply lines. Devices were fabricated using manufacturing certified assembly lines or on manufacturing certified instrumentation. The devices were tested using archived digital ECG recordings certified by a panel of cardiologists [8], and by recording ECG signals from a human volunteer. All fabricated devices properly detected and reproduced archived ECG signals at the host computer, and the calculated heart rates and heart rate variations were in close agreement with the analysis of the certified signals. Human ECG signals were detected, communicated to the host and analyzed for heart rate and heart rate variation for a volunteer at rest, and during mild exercise and cool down. Reliability issues included cracks in the copper traces and variable resistance in the printed gold-copper tab interfaces.

II. Design of HPM Electronics & Software

The design requirements of the HPM in terms of the functional requirements, form factor (to fit into a flexible substrate at most 2 inches square) and endurance on battery power were the primary drivers behind the selection of the electronic components. The HPM specifications called for the acquisition of ECG signals in real-time, to send them out on a wireless link for display and analysis on an external host, and to provide up to 30 hours of lifetime on a single non-rechargeable battery. This specification, in turn, led to the following design requirements:

1. The data must be transmitted from the HPM to the host in digital form for reliability. This dictates the use of an analog-to-digital converter (ADC) on the HPM itself.

2. A secure communication link between the host and the HPM, since the privacy of the subject needs to be preserved.

3. A minimum of 12-bit resolution is needed on the ADC to meet the clinical requirements for ECG signals prior to display and analysis.

4. The entire HPM electronics should consume very little energy to support the use of non-rechargeable batteries that comply with the form factor requirements of the HPM.

5. The HPM must use a minimum number of electrodes for sensing the ECG signals.

6. The HPM must also comply with the safety requirements associated with any device placed for an extended duration on the subject's body.

Contemporary wireless communications chips consume a relatively large amount of power compared to data and pre-processing chips, acquisition and ADC. Furthermore, such wireless devices are also capable of transmitting data at a rate much higher than the rate at which ECG signals are acquired. To meet Requirements (2) and (4), it is clear that continuous operation of the transmitter on the HPM will drain the battery too rapidly and thus, fail to meet Requirement (5). The ECG data acquisition should proceed continuously and large chunks of acquired ECG data need to be buffered into memory on the HPM prior to their transmission to the host. To permit ECG data acquisition and transmission, at least two sets of RAM buffers are needed - one to buffer the data as it is acquired and another to store previously acquired data for transmission to the host. With this arrangement, the buffered data can be quickly transmitted to the host and the transmitter can be shut off to save power until enough data is acquired and buffered for the next transmission. Having larger buffer capacities on board the HPM, up to a limit, will clearly help in conserving power that would be otherwise spent by operating the transmitter more frequently, but still sending the data at appropriate intervals.

The choice of the wireless communication protocol was also narrowed down to Bluetooth after ruling out Wi-Fi, special band RF and Zigby as potential candidates, since the low power Bluetooth implementations provided the least power requirements.

The component choices for the electronics ranged from the use of separate chips for the ECG signal processing, ADC, microcontrollers, storage and wireless interface to chips that implemented multiple functions within a few chips. Ideally, a single chip solution would be desirable but no existing off-the-shelf product provided that capability.

Two chips were eventually selected for the HPM prototype:

• TI CC2540: This is a system-on-a-chip (SoC) that integrates an analog multiplexer, a 12-bit ADC, an 8-bit microcontroller, RAM, EPROM, an encryption engine, a Bluetooth transmitter and receiver and analog and digital IO ports. The functions that can be implemented with this SoC meet Requirements (1) through (4) with proper software support.

• AD8232: This is a special function chip that is designed to process and filter out noise from ECG signals acquired from 2 or more electrodes.

Fig. 1 depicts how these chips are used in the HPM prototype. The final Phase I prototype actually replaces the CC2540 with a BLE module that includes the CC 2541, crystals used for the clock generators and passive

components associated with the Bluetooth antenna, reducing the parts count considerably.
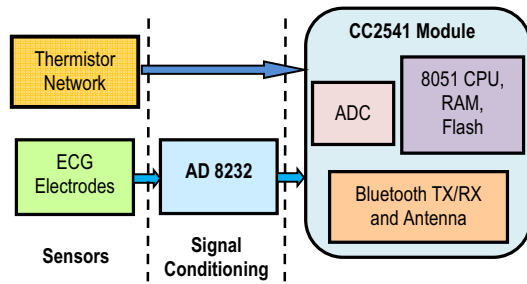
Figure 1: Schematic of components and circuits.

The HPM prototype employs two different sensors: a two lead sensor on the flexible substrate to sense ECG signals and printed thermistors to sense the body temperature. The 8232 was configured to operate on the two-electrode ECG input, without requiring any other connections to the subject's body.

A significant amount of effort was expended to reduce the overall power requirement of the HPM. First, the Bluetooth power requirement was reduced by using a software sequence to determine the minimum power setting at which the transmitter could be operated at while keeping the communication with the host reliable. Second, multiple buffers were used to shut down the transmitter after filled buffers were transmitted and until the next buffer was ready for transmission. Third, significant code optimizations were performed to reduce the power draw during data acquisition. Fourth, to increase the endurance of a single battery, a variable duty cycle operating mode was implemented: the HPM can be operated in alternating cycles of an active and a passive phase. In the active phase, the HPM continuously acquires and sends data while in the passive phase it is put into the deep sleep state, conserving power. The HPM can enter this state automatically when the battery power drops or when the acquired ECG signal changes slowly. Finally, the thermistor measurement circuitry, which was designed to provide a reliable reading without needing a stable voltage source, was activated only during temperature measurements to save power.

The requirement of using a non-rechargeable battery left little choice in selecting an appropriate battery. A button cell, which provides the highest power density in the specified form factor, was the only viable choice. These batteries experience a significant capacity reduction when large current surges occur - as it does during the activation and use of the Bluetooth transmitter. In an attempt to reduce such current surges, a large capacitor was used to provide the added charge supply when needed without straining the battery.

The physical design of the HPM prototype took into consideration fabrication issues as well as the requirements of the form factor and Requirement 6. The electronic components were all mounted on one side of the flexible substrate (using etched wiring patterns) while the sensors (single-lead ECG electrodes) and the thermistor were mounted on the other side, remaining in contact with the subject's body. A ground plane was also used to shield the subjects from the Bluetooth signal and prevent noise injection into the ECG signal chain. The ECG electrodes were printed in gold, making contact with etched patterns that connected the leads to the sensing circuitry on the other side through via connections. Similar THVs connections were used to connect the printed thermistors to the sensing circuitry.

III. FABRICATION

A. Substrate

First, Initially it was thought that fabrication of the Biometric Human Performance Monitor (BHPM) would require that a circuitized polyimide (PI) Kapton®HN substrate with attached electrical components, and a second polyethylene napthalate (PEN) substrate with ink-jet printed sensors, would need to be fabricated independently and subsequently electrically interconnected. This was because a process for ink jet printing on PI was not yet been defined. However, a process flow was developed for copper circuitization and sensor printing on a single polyimide substrate. This process is described below.

Fig. 2 shows the construction for integrating printed sensor electronics with photolithographically defined and electroplated copper circuitry. Copper traces and pads were concurrently defined at i3 Electronics using photolithographic techniques and a semi-additive plating process on both surfaces of the double-sided PI flexible substrate. Here, all copper circuit lines and pads were two microns thick. Electrical interconnection between the two circuitized sides was achieved using plated THVs formed using a high-precision ultraviolet (UV) laser drilling system. Gold ECG electrodes and metal-polymer thermistors were then ink-jet printed at the University of California (UC) at Berkeley on the sensor side (opposite side) of the flex. Electrical interconnection between the gold and copper circuits was achieved by overlapping gold onto copper capture pads. The flexible substrates were then sent back to i3 Electronics for soldermask application and soldered-components attach.
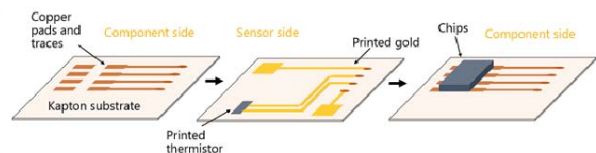
Figure 2: Schematic of manufacturing process flow.

Fig. 3. Is a schematic representation of cross-section of the BHPM. Copper traces and pads were defined using photolithography on the component and sensor sides of the substrate. Then sensors were printed on the sensor side of the flexible patch. Finally, soldermask, analog, digital, and battery holder components were solder-attached on the component side of the board.
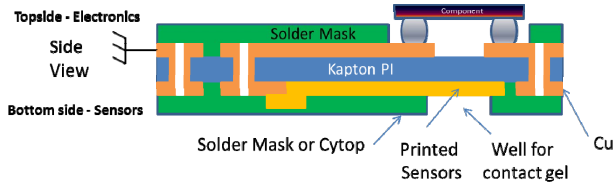
Figure 3: Schematic cross-section that illustrates the vertical materials stack-up and features in the BHPM.

The double-sided flexible hybrid BHPM is shown schematically in cross-section in Fig. 3. The two copper circuit layers are shown interconnected by THV's which provide electrical interconnection from the electronic components side to the sensor side on which the ECG and thermistor sensors are printed. It is this bottom (sensor) side that is in contact with the skin of the wearer.

A schematic of the component layout is shown in Fig. 4. Placement of the CR2032 battery is in a corner of the HPM patch not populated by ECG electrodes on the opposing (sensor) side of the flex. Ink-jet printed gold circuit traces and electrodes, as seen through the part from the component side, are shown in green.
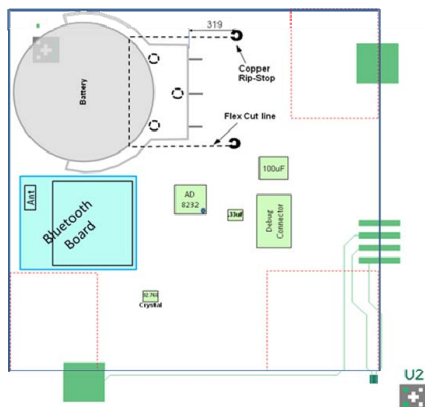
Figure 4: Schematic component layout for the BHPM as viewed from the component side of the module.

Fig. 5 shows a photograph of the finished product – the FHE BHPM. The component side shown in Fig. 5a holds the traditional silicon-based hard electronic components and includes the battery holder. Fig. 5b shows the sensor side, where the gold ECG electrodes and the thermistor are visible. This construction yielded a true FHE sensing device.
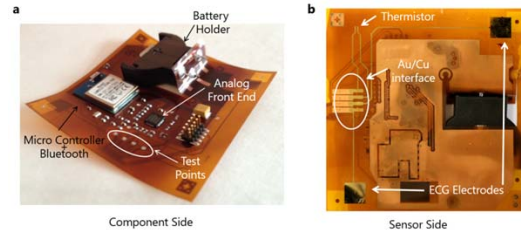
Figure 5: Photographs of both the component (a) and sensor (b) sides of the BHPM device.

B. Inkjet-Printed ECG Electrodes

Inkjet printing is a digital and versatile printing method, which allows agile sensor design and fabrication [10]. Additionally, inkjet printing allows deposition of high-purity, solution processable materials with spatial resolutions on the order of tens of microns [11,12] Therefore, inkjet printing was chosen for the sensor fabrication. As for sensor materials systems, gold was used for the electrodes due to its superior chemical inertness to biological fluids and living tissues [13,14]. After inkjet printing the gold nanoparticle ink, electrodes are formed by an annealing step that fuses the gold nanoparticles and yields conductive traces. During the printing step, the surface energy of the substrate is an important parameter; higher than optimum surface energy results in ink spreading and lower than optimum surface energy results in dewetting of the printed ink. Printing on Kapton HN polyimide that is used for flex circuit board fabrication, proved challenging because the surface energy of Kapton is not optimized for printing. The most commonly used substrate for printed electronics is poly(ethylene napthalate) PEN substrate, which has contact angle in the range of 80-90°. The surface energy of the PEN associated with this contact angle (with deionized water) has been found to be ideal for inkjet printing. Kapton HN polyimide has a contact angle in the range of 40-50°, indicating a much higher surface energy than is acceptable for printing. However, a series of plasma surface treatments can be employed to reproducibly tune the surface energy of the Kapton to what is ideal for inkjet printing. Tetrafluoromethane (CF_4) plasma and a subsequent oxygen (O_2) plasma treatment were employed for optimizing the surface energy of Kapton.

The process flow for fabricating the electrodes is shown in Fig. 6a. CF_4 and O_2 plasma treatments are performed to tune the surface energy of the Kapton substrate for reliable and reproducible inkjet printing. Then gold nanoparticle ink is printed using a Dimatix inkjet printer. After sintering the ink at 230° C for an hour, an amorphous fluoropolymer (Cytop) is spin-coated to encapsulate the traces. The 100 nm Cytop covering proved to be a robust encapsulation and did not hinder electrode-skin contact. Then the electrodes are exposed using O_2 plasma etching so that only the electrodes contact the skin. Electrode gel is used for a robust electrode-skin contact. Fig. 6b shows the fabricated electrodes. While multiple electrode layout design iterations were performed,

this design utilized 4 electrodes placed along two sides of the substrate, aiding the system software to optimize a pair of electrodes that yield the maximum signal strength. The histogram in Fig. 6c shows the reproducibility of the process verified using electrical resistance data. We observed a mean sheet resistance of 0.36 Ω/sq for a 600 nm thick circuit line. The electrodes demonstrated strong adhesion to Kapton as seen in the bending test data for 1000 cycles (Fig. 6d). The bending test was performed at a bending radius of 5 mm. Data for two different traces are shown in the plot; most of the noise in the data is instrumentation noise.
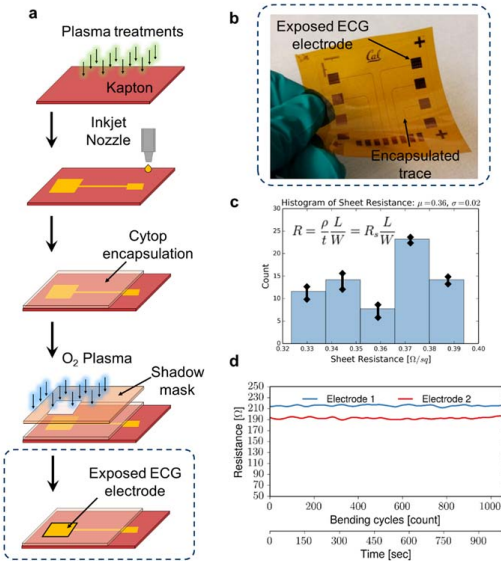
Figure 6. Fabrication and characterization of printed gold ECG electrodes on Kapton. (a) The fabrication process of printed electrodes. Plasma treatments are performed to tune the surface energy of the Kapton substrate for reliable and reproducible inkjet printing. Then gold nanoparticle ink is printed using an inkjet printer. After sintering the ink, an amorphous fluoropolymer (Cytop) is spin-coated to encapsulate the traces. Then only the electrode area is exposed using O_2 plasma etching. Electrode gel is applied on top of the electrodes for robust electrode-skin contact before taking human measurements. (b) Photograph of the printed electrodes on Kapton. The exposed electrodes and the encapsulated traces are shown. (c) The sheet resistance of the printed electrodes. 60 electrodes from 5 batches (n = 300) were measured, and a mean sheet resistance of 0.36 Ω/sq. was obtained. The error bars represent the standard deviation of the data. (d) The electrodes were bent to a 5 mm bending radius. Minimal change in the resistance of the electrodes was observed during the bending test.

IV. BHPM TESTING AND PERFORMANCE

We initially evaluated our ECG circuitry by connecting a set of printed gel based ECG electrodes to a breadboard version of the circuitry and placing the electrodes on the chest of a human volunteer. The ECG signal was processed and transmitted from the breadboard to a Bluetooth host. These signals were essentially the same as those acquired from a pair of clinical ECG electrodes connected to a standardized commercial belt worn single lead ECG monitor. The traces were recorded from the same subject within a few minutes of each other. All measurements on human volunteers were done in compliance with procedures approved by the Binghamton University Internal Review Board under protocol #3267-14.
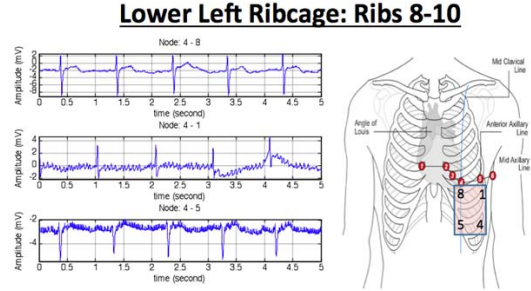
Figure 7: Location of ECG electrodes in the area of ribs 5-7 and the resultant signals between three electrodes pairs.

Fig. 7 shows the location of ECG electrodes in the area of ribs 8-10 and the resultant signals between three electrodes pairs. The next series of tests optimized the location of the electrodes on the volunteer's chest. The electrodes we placed in many locations on the center of the chest, including the classic V1-V2 positions, and all along the left side of the rib cage on the front, side and back. The highest and quietist signal levels were recorded from the region of ribs 8 to 10 (Fig. 7). In this position, the highest signals were recorded when the electrodes were at positions 4 and 8 in Fig. 7. In this configuration, the electrodes are on the diagonal of the BHPM and are aligned to the heart axis running from the upper right atrium through the lower left ventricle. The other two electrode pairs were aligned at a considerable angle to this axis and showed lower level signals with more noise.

These breadboard tests demonstrated the operation of a single lead ECG using gel based printed electrodes on a 2x2" patch. The circuitry was then transferred to Kapton substrates. Before testing on human's all BHPMs were evaluated using certified archived ECG signals applied to the test points on the component side of the substrate. These signals are well-characterized human ECG recordings that have been analyzed and certified by a group of cardiologists, and are available at the MIT-BIH arrhythmia database [8]. All tested devices performed with the same high fidelity, producing signals at the host that were comparable to the input signals. The calculation of heart rate variation parameters from these signals compared favorably to the certified values. These results show that the BHPMs detected, filtered, and communicated the archived signal to

the Bluetooth host with high reproducibility. This test is considered to be the gold standard with respect to the operation of the ECG circuitry and the communications. Typical archived results are shown in Fig. 8. The signal at the host showed less noise than the archived signal input and even lower noise after peak detection on the host. Calculation of the heart rate variation parameters were comparable to those listed in the certified database. These parameters were the mean of the time interval between peaks (MI), the standard deviation (SD) of the peak intervals, the root mean square of the standard deviation (RMSSD), and the percentage of peak intervals that exceeded 50 msec (%RR50).

	MI (ms)	SD (ms)	RMSSD (ms)	%RR50
BHPM	951.8519	59.9444	65.2890	42.50%
Archived	951.7490	60.1043	65.6491	43.75%
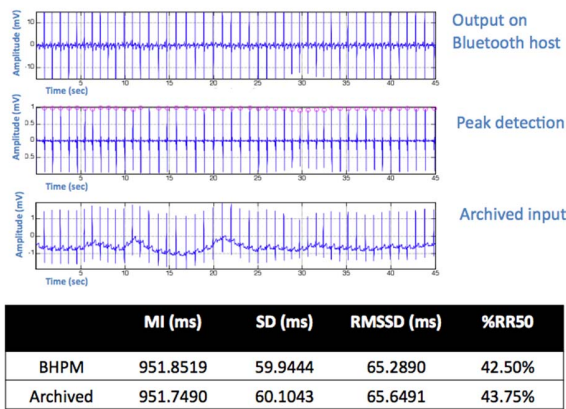
Figure 8: BHPM signal at the Bluetooth host for an archived ECG signal input, and the clinical parameters derived from both signals. The upper left ECG trace is the BHPM signal after the first stage of amplification and low frequency filtering, the middle trace is the BHPM signal with red circles depicting detected peaks after the second stage of amplification and high frequency filtering, and the bottom trace is the inputted archived signal.

BHPMs were then used to record ECG signals from human subjects, and in two cases recordings were taken when the subject was at rest, during mild exercise, and cool down. The BHPM was attached to the lower left rib cage with hypoallergenic medical tape. The BHPMs demonstrated high-quality ECG traces at the Bluetooth host with essentially perfect peak detection and with clinical calculations from the signals that were representative of the clinically normal subjects. The heart beat rate showed appropriate variations corresponding to whether the subject was at rest or was exercising (Fig. 9). The upper ECG trace shows the typical high frequency noise including spikes with amplitudes equal to or greater than the ECG peaks, but as seen in the peak detection trace the filtering eliminated this noise and every peak was detected by the peak detection algorithm. The plot of the heart rate follows the status of the volunteer from rest to mild exercise to cool down.
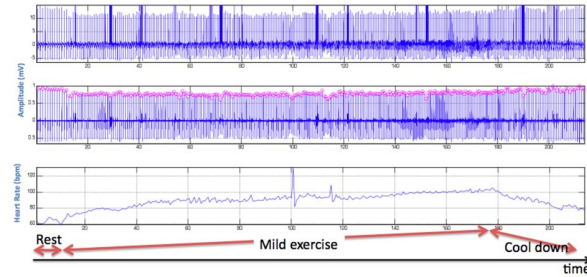
Figure 9: Heart beat rate corresponding to whether the subject was at rest or was exercising.

V. RELIABILITY TESTING

All manufactured BHPMs were tested after assembly using archived ECG signals, and were found to produce high-quality ECG outputs at the Bluetooth host that were essentially indistinguishable from the certified archived input signals. This verified the transition of the ECG and communications circuitry to the Kapton substrate. Four BHPMs were tested on human subjects and found to produce high-quality ECG signals at the host that demonstrated appropriate clinical parameters. Two BHPMs recorded and communicated ECG signals from subjects at rest and during mild exercise. Nine of the BHPMs failed to operate subsequent to handling and functional testing. Seven of these failures were associated with the analog preconditioning chip portion of the circuit; all these failures appeared to be due to mechanical failure upon repeated flexure. Two units failed due to communication issues with the Bluetooth module.

One of the units that functioned properly during the mild exercise routine was tested on a bend tester for 200 cycles on a 4" mandrel. This mandrel was selected as it represents a smaller radius of curvature than that encountered on the chest of an adult human. An archived ECG signal was inputted to the unit before and after cycling on the bend tester and the results at the Bluetooth host were essentially identical. Representative ECG traces are shown in Fig. 15 at the end of this paper. The preliminary conclusion is that bending the unit over a 4" radius of curvature is not detrimental to the functioning of the BHPM. Further testing along these lines with a larger number of units and with mandrels of smaller radii of curvature is needed.

Seven assembled BHPM units demonstrated similar failures associated with the 8232 analog signal preconditioning chip region of the circuit, and were characterized as a total loss of signal at the Bluetooth host, i.e. the signal went to zero with no amplification of noise. This indicated either a loss of output or input signal, or power to the 8232 or some combination of these conditions. It was noted that slight pressure applied to the chip reestablished operation indicating that a broken contact or circuit trace on the substrate was likely the cause of the failure. The analog processing chip and some of its associated circuitry is show in Fig. 10. The chip has five soldered connections on each side of the chip.
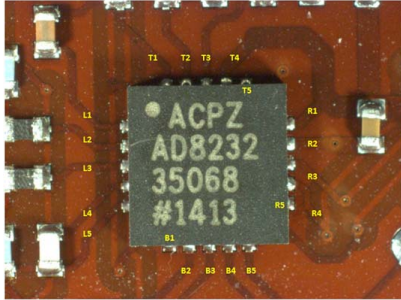
Figure 10: Optical image of the AD8232 chip assembled to the flex circuit.

Pressing on this chip resulted in intermittent electrical functioning of the HPM flex circuit that was otherwise nonfunctional. Individual circuits are labeled with yellow alpha-numeric identifiers. Light microscopy of the solder joints showed no evidence of defects, and subsequent x-ray and confocal scanning acoustic microscopy (CSAM) did not identify cracked or broken solder joints.

High magnification light microscopic viewing from the component side of the substrate using transmitted light through the sample, without any top illumination, revealed very fine breaks in the circuit lines leading from the attachment pads. This break is visible in Fig. 11. The bright clear area around the copper tab and a short section of the trace is due to light transmission through the Kapton substrate alone. The surrounding somewhat darker area is covered with solder mask. The crack in the trace is almost exactly aligned with the edge of the window in the solder mask.
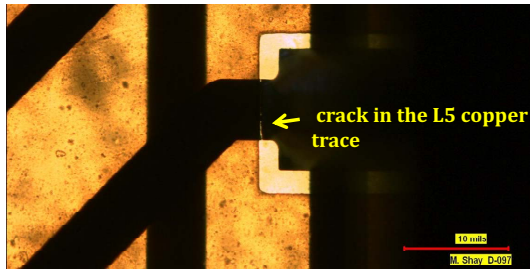
Figure 11: Optical image of backlit circuitry and components on a failed part. A crack in the trace is visible.

When the unit is imaged from the sensor side using top illumination a reflected light image of the same area of copper is viewed through the Kapton substrate. The tab areas of L4 and L5 revealed low contrast anomalies transecting the circuit lines along the soldermask edge as seen in Fig. 12. The conclusion is that the anomaly is a reflection from the copper line that has been flexed so that a puckered region of copper has been formed. This defect appears to precede fracturing of the copper traces as no crack was observed in L4. This adds support to a suspicion that the circuit opens may be the result of flexure of the copper at the

soldermask/solder interface, where the copper is structurally the weakest.
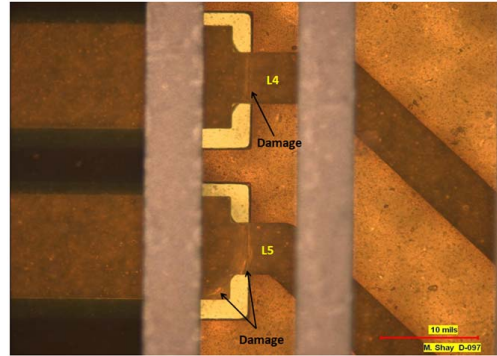
Figure 12: Top illumination, liquid-enhanced image, taken from the sensor side (ground plane) side of the circuit revealing damage to the underside copper of the L4 circuit as well as the L5 circuits and pads

The T1-T4, R1-R5, and B1-B5 circuit lines and respective pads are also shown in Fig. 10; however, possible breaks in these lines are not visible due to the presence of ground plane copper on the sensor side preventing light transmission.

Simple wet hand-sanding removed the ground plane allowing backlighting to evaluate all the other component-side copper circuits and pads. Backlight evaluation of the remaining circuits showed additional circuit lines were completely or partially cracked Fig. 13 as shown below and continued in the next column.
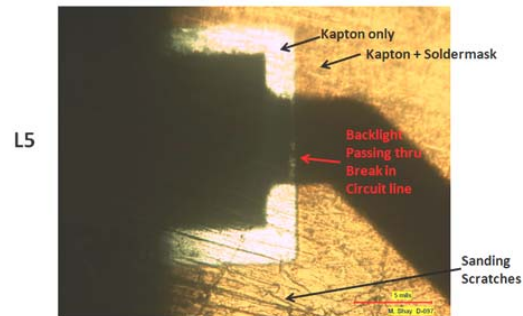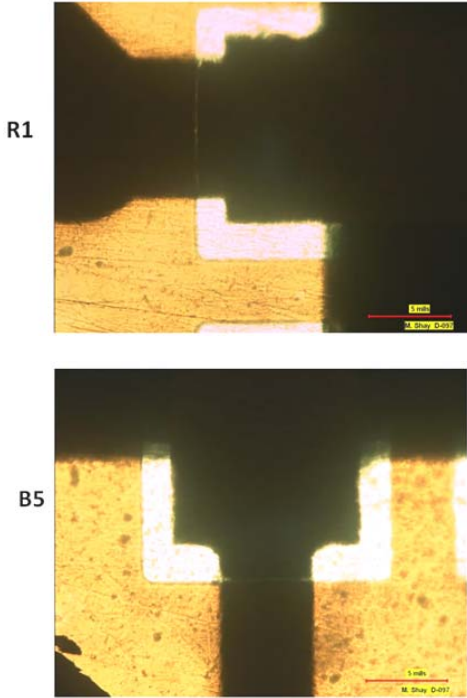
Figure 13: Backlit component attach circuits and pads after ground plane copper (sensor side) was removed by wet sanding. Break in L5 is clearly seen again as a vertical white line, while breaks in L1, R1, and B5 circuits, and partial breaks in T1, L2, L3, L4 circuits are also revealed (those figures were omitted.)

Thus, there were multiple circuit lines that had formed both through-fractures as well as partial fractures. In all cases, the locus of the failure is very close to the soldermask edge of the copper circuit line. We believe this is because it is the transition point from the highly-rigid solder-filled pad held strongly in-plane by the die during flexure, to a thin $2\mu m$ thick copper trace. In many cases, as the solder reaches the soldermask edge the soldermask is lifted slightly and allows some solder wicking beneath it. This makes the transition from fully-rigid to flexible somewhat more variable; however, the breaks in the copper clearly occur where there is the least resistance to bending in the x-section. Circuit line breaks occurred mainly on the side of the chip with the least continuous ground plane coverage, where the circuits approach the component pads over Kapton only (without ground plane present), and are closest to the assumed origination of strain. We believe this indicates that repetitive bending induced a significant flex-fatigue of the copper circuits.

The other reliability issue encountered was a higher and more variable resistance than expected in the circuit path from the ECG electrodes. This includes gold and copper traces, the interface between the printed gold and the copper pads, and the THVs (Fig. 14). Trace 1 is considerably longer than trace 2. Light microscopic imaging of the intact units showed no defects. However, the variation in the resistance measurements is shown in Table 1.
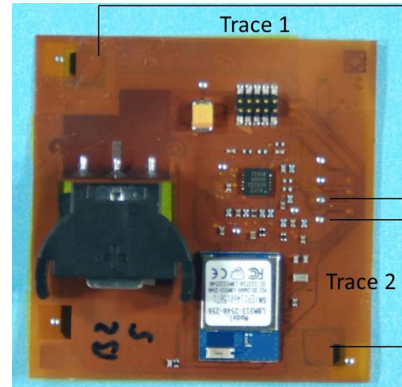
Figure 14: Circuit paths between the gold printed electrodes and the component side.

Thus, some cross section studies of the traces including the THVs and the Au/Cu interface were conducted. Light micrographs of the cross section of the double-sided copper features and a copper plated THV showed that the copper features and plating were intact and should have good electrical continuity. The plating thickness in the THV is approximately the same thickness as the surface copper features on both sides of the substrate, and the corners are well formed and of the same copper thickness. The Kapton is seen as a uniform featureless structure, as opposed to the soldermask which a different density with some internal features. Both are easily discerned from the potting epoxy.

Part #	Resistance (t1 r1)	Resistance (t1 r2)	Resistance (t2 r1)	Resistance (t2 r 2)
N3A2	84	Open	Open	Open
N3B2	71	72	30	30
N4A3	78	75	40	40
N4B1	78	78	NA	NA
N5A2	92	106	44	46
N5B1	79	79	38	37
N5B2	122	122	38	38
N8A2	131	131	50	51
N8B2	59	49	19	19

Table 1: Comparison of electrode to component side circuit resistances measured on nine units.

REFERENCES

[1]   M Garg, Q Gui, J Turner, K Ghose, Z Jin, M Poliks, S Czarnecki, Y. Khan, A. C. Arias, F. Egitto, M. Schadt, R. Welte, P. Hart, Wearable Flexible Hybrid Electronics Monitor for Recording Human

Biometrics, FlexTech 2015, FlexTech Alliance Meeting, Monterey, CA, February, 23 – 26, 2015.

[2] Y. Khan, A. C. Arias, M. Garg, Q. Gui, J. Turner, K. Ghose, Z. Jin, M. Poliks, S. Czarnecki, F. Egitto, M. Schadt, R. Welte, P. Hart, Interfacing Printed Sensors to Conventional Electronics for Wearable Sensor Patch, FlexTech 2015, FlexTech Alliance Meeting, Monterey, CA, February, 23 – 26, 2015.

[3] P. Salvo, R. Raedt, E. Carrette, D. Schaubroeck, J. Vanfleteren, and L. Cardon, "A 3d printed dry electrode for ecg/eeg recording," Sensors and Actuators A: Physical, vol. 174, pp. 96–102, 2012.

[4] J.-Y. Baek, J.-H. An, J.-M. Choi, K.-S. Park, and S.-H. Lee, "Flexible polymeric dry electrodes for the long-term monitoring of ecg," Sensors and Actuators A: Physical, vol. 143, no. 2, pp. 423–429, 2008.

[5] A. Searle, and L. Kirkup, "A direct comparison of wet, dry and insulating bioelectric recording electrodes," Physiological Measurements, vol. 21, no 2, 271-283, 2000.

[6] Y. M. Chi, S. R. Deiss, and G. Cauwenberghs, "Non-contact low power eeg/ecg electrode for high density wearable biopotential sensor networks," in Wearable and Implantable Body Sensor Networks, 2009. BSN 2009. Sixth International Workshop on. IEEE, 2009, pp. 246–250.

[7] A. Serteyn, R. Vullings, M. Meftah, and J. W. M. Bergmans, "Motion Artifacts in Capacitive ECG Measurements: Reducing the Combined Effect of DC Voltages and Capacitance Changes Using an Injection Signal". IEEE Trans. on Biomedical Engineering, Vol. 62, No. 1, January 2015.

[8] Archived ECG signals and heart rate variability data are from: https://www.physionet.org/physiobank/database/ptbdb/

[9] S. Lee, J. Hong, C. Hsieh, M. Liang S. C. Chien, and K. Lin, "Low-power wireless ECG aguistion and classification system for body sensor networks," IEEE J. Biomed. and Health Informatics, vol 19 no 1, 2015, pp 236-246.

[10] M. Singh, H. M. Haverinen, P. Dhagat, and G. E. Jabbour, "Inkjet printing-process and its applications," Adv. Mater., vol. 22, no. 6, pp. 673–685, 2010.

[11] A. C. Arias, J. D. MacKenzie, I. McCulloch, J. Rivnay, and A. Salleo, "Materials and applications for large area electronics: Solution-based approaches," Chem. Rev., vol. 110, no. 1, pp. 3–24, 2010.

[12] Y. Khan, A. E. Ostfeld, C. M. Lochner, A. Pierre, and A. C. Arias, "Monitoring of Vital Signs with Flexible and Wearable Medical Devices," Adv. Mater., Feb. 2016.

[13] Y. Khan, F. J. Pavinatto, M. C. Lin, A. Liao, S. L. Swisher, K. Mann, V. Subramanian, M. M. Maharbiz, and A. C. Arias, "Inkjet-Printed Flexible Gold Electrode Arrays for Bioelectronic Interfaces," Adv. Funct. Mater., vol. 26, no. 7, pp. 1004–1013, Feb. 2016.

[14] S. L. Swisher, M. C. Lin, A. Liao, E. J. Leeflang, Y. Khan, F. J. Pavinatto, K. Mann, A. Naujokas, D. Young, S. Roy, M. R. Harrison, A. C. Arias, V. Subramanian, and M. M. Maharbiz, "Impedance sensing device enables early detection of pressure ulcers in vivo.," Nat. Commun., vol. 6, p. 6575, 2015.
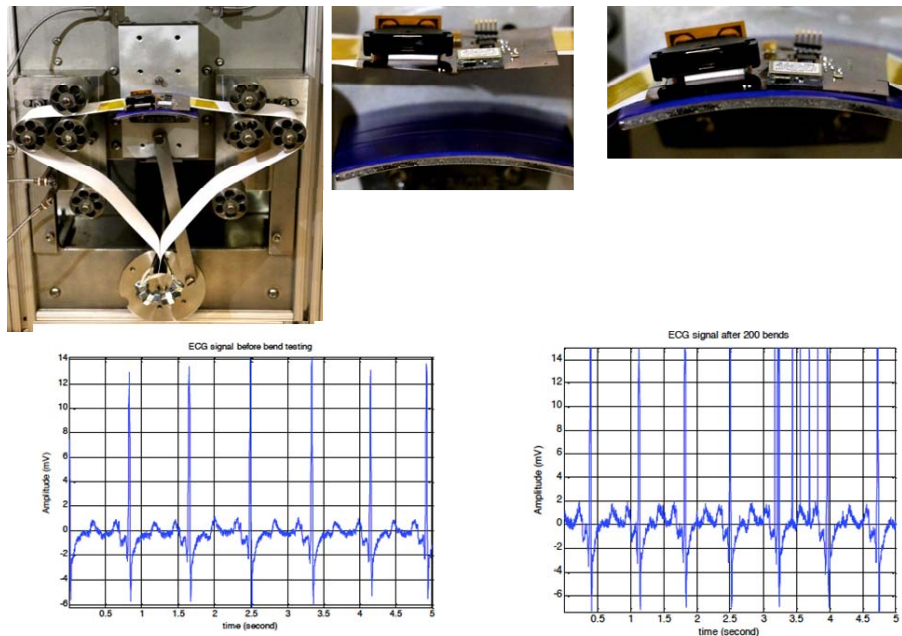
Figure 15: Depicts the bend apparatus with a BHPM mounted in the upper left hand image. The upper middle image shows the BHPM when the mandrel was at its lowest vertical position and the upper right image shows the BHPM when the mandrel was at its highest vertical position. The left ECG trace is the signal at the host before bend testing and the right trace is the signal after 200 cycles. The noise peaks between 2.25 and 4.0 seconds in the right trace are typical of ECG systems and are filtered out by the electronics.